Ionic self-assembled derivatives of perylenetetracarboxylic dianhydride: facile synthesis, morphology and structures†

Guihua Fu,[a] Muli Wang,‡[a] Yongliang Wang,[a] Nan Xia,[a] Xinjun Zhang,[a] Miao Yang,[a] Ping Zheng,[a] Wei Wang*[a] and Christian Burger*[b]

Received (in Durham, UK) 21st October 2008, Accepted 20th November 2008
First published as an Advance Article on the web 15th January 2009
DOI: 10.1039/b818650b

A facile ionic self-assembly method was used to synthesize technologically important derivatives of perylenetetracarboxylic dianhydride (PTCDA). This extremely facile one-pot synthesis was performed in water and provided relatively pure complexes precipitated from water in high yield at room temperature. This is particularly interesting because the synthesis of most PTCDA derivatives using conventional methods often requires relatively complicated and harsh conditions. The self-assembly of the complexes was studied under different conditions. In ethanol–water or toluene–acetone binary solvents, long aggregates in the range of micrometers were obtained. Through a slow evaporation of toluene, one of the complexes can form ultralong aggregates, up to ~4 mm in length. The structural packing of these systems is dominated by the stacking of the rigid perylene disks, embedded in an aliphatic soft matrix that may or may not crystallize, as evidenced by X-ray diffraction (XRD). Details of the structural packing such as layer spacings and perylene tilts also determine different fluorescence functionalities.

Introduction

Nowadays it is well known that owing to low charge mobility and exciton diffusion length the performance of most organic semiconductors is significantly poorer than that of commonly used inorganic semiconductors. This may be one of the main obstacles limiting their application as key functional materials in optical and electronic devices. Fortunately, recent studies have demonstrated that constructing highly ordered structures, particularly one-dimensional (1D) columnar nanostructures, of organic and polymeric semiconductors can be an efficient approach to enhance their performance and to extend their application into optoelectronic materials.[1,2] This is because in 1D columnar nanostructures stacked planar aromatic molecules exhibit π–π interactions which increase the overlap between the electronic wave functions of neighboring molecules,[3] thereby leading to a high charge-carrier mobility in these nanomaterials along the long axis of the nanostructure.[1d,4]

As important industrial dyes and pigments as well as, in recent years, very promising organic semiconductors, a great number of derivatives of 3,4,9,10-perylenetetracarboxylic dianhydride (PTCDA) have been developed to increase their solubility in common organic solvents and/or to decrease their melting point.[5] Three major methods have been utilized to modify PTCDA: The first method is a well developed way in which PTCDA reacts with aromatic or aliphatic amines to create perylene tetracarboxylic acid diimides (PTCDIs), the most important derivatives of which structures and properties have been extensively studied.[5] The second method is to prepare perylene tetracarboxylic tetraesters (PTCTEs) *via* esterification of PTCDA.[6] The final method is to introduce substituents at the carbocyclic scaffold in the so-called bay-area to change the performance of the perylene core.[7] Most PTCDA derivatives have demonstrated the potential to construct diverse supramolecular structures, mainly because of the strong π–π interaction of the perylene cores.[8–14] In order to further increase the abundance and diversity of these nanostructures and to further control their functionality, various functional groups were introduced into these compounds in which hydrogen bonding,[9] electrostatic,[10] hydrophilic,[11] amphiphilic,[12] metal–ligand[13] and other[14] interactions play important roles in the self-assembly into nanostructured materials. Nanoscale fibers, wires, tubes, belts/ribbons have been formed *via* self-assembly in organic media and lyotropic or thermotropic liquid crystal phases with columnar or smectic arrangements have been observed in their bulk samples. Existing synthesis methods for these PTCDA derivatives require complex and harsh conditions, such as high reaction temperatures, long reaction times, organic solvents (*e.g.* pyridine, imidazole, quinoline, isoquinoline *etc.*) and, often, the yield is relatively low. Thus, developing a facile one-pot method to synthesize novel PTCDA derivatives with the ability to form ordered structures should be very welcome to most synthetic chemists in this field.

It has been demonstrated that ionic self-assembly (ISA) is a facile and efficient method to build up novel functional materials by complexing two different building blocks with opposite charges *via* electrostatic interactions.[15] This

[a] *The Key Laboratory of Functional Polymer Materials of Ministry of Education and Institute of Polymer Chemistry, College of Chemistry, Nankai University, Tianjin, 300071, China. E-mail: weiwang@nankai.edu.cn*
[b] *Chemistry Department, Stony Brook University, Stony Brook, NY 11794-3400, USA. E-mail: cburger@sunysb.edu*

† Electronic supplementary information (ESI) available: ^{1}H NMR, FTIR spectra and the results of PTCT-DHAB. See DOI: 10.1039/b818650b

‡ Current address: Hengyi Research Institute, Yaqian Town, Hangzhou City, Hangzhou, Zhejiang 311209, China.

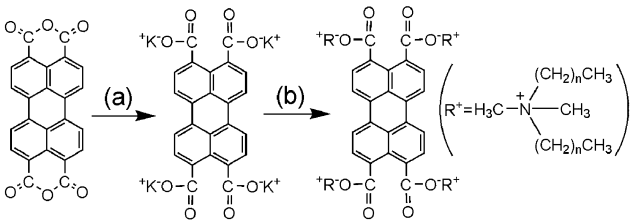

Scheme 1 Synthesis process and chemical formulas of PTCT-DOAB and PTCT-DHAB complexes.

technique allows stoichiometric precipitation of starting materials in aqueous solution without other byproducts and, thus, the isolation of the pure complex in high yield *via* simple filtration. ISA has been used for the preparation of polyelectrolyte-surfactant complexes[15a,b] and for complex formation with other charged species such as perylenes or certain dyes,[10,15c,16] thereby creating highly ordered nanostructured materials with interesting functionalities. In these works, PTCDA was first transformed into the diimides PTCDI by reaction with functionalized amines, followed by a reaction at the introduced functional groups to obtain the ionized PTCDI derivatives, which can be finally complexed with oppositely charged surfactants to produce ISA functional materials containing perylene cores. It would be an advantage if PTCDA derivatives could be synthesized directly from PTCDA *via* the ISA method in "green" media, such as water, without extra purification.

Herein, we report a facile one-pot synthesis of a novel type of PTCDA derivative *via* ISA. Our aim is to avoid the synthesis of intermediate PTCDA derivatives in organic media. The starting materials were the potassium salt of 3,4,9,10-perylenetetracarboxylic acid (PTCTK, prepared from a simple treatment of PTCDA with aqueous potassium hydroxide) and commercially available cationic surfactants with two long alkyl side chains: dioctadecyldimethylammonium bromide (DOAB) and dihexadecyldimethylammonium bromide (DHAB). Adding neat DOAB or DHAB aqueous solutions dropwise to PTCTK aqueous solution immediately yields precipitates of the complexes formed by PTCT with DOAB or DHAB, denoted as PTCT-DOAB or PTCT-DHAB, respectively (Scheme 1). In the present work, we will study their solubility and focus on the ordered structures formed by self-assembly during the synthesis and reconstituted in solutions with various mixed solvents. The correlation between the ordered structures and fluorescence was also studied. Since PTCT-DHAB has almost the same structure and properties as PTCT-DOAB, its results are summarized in the supplementary information (ESI†).

Results and discussion

Synthesis and chemical structure characterization

This facile one-port synthesis is particularly interesting as it can be completed within 1 h in water or a mixture of water and alcohol which are both more environment-friendly than most organic solvents. These new perylene derivatives could be obtained with high yield at room temperature. In comparison with other perylene derivatives, such as perylene tetracarboxylic diimides (PTCDIs), the synthesis of PTCT-DOAB (or PTCT-DHAB) has the following advantages: Low temperature (room temperature), short reaction time (<1 h), high yield (>97%), simple treatment process, and no organic solvents used in the reaction. The formation of the charge-stoichiometric complex was at first evidenced by ^{1}H NMR spectroscopy. To assess the purity of the complexes in terms of remaining traces of K or Br, an elemental analysis was performed; 0.02 wt% K^+ was found and no Br^- was detected. Accordingly, one K^+ was calculated to be in every 59 complex molecules (one non-complexed charge site per 59 PTCTK molecules) and no (or at least undetectable) absorbed Br^-, indicating that all free surfactant has been removed from the complex. This shows that the complex is very pure with a one-to-one charge-stoichiometric complexation ratio.

PTCTK was soluble in water, and DOAB was soluble in ethanol–water binary solvent. When they were mixed, ionic bonds formed due to the attractive electrostatic interaction between O^- and N^+, leading to an overall charge-neutral complex. Because of the strong hydrophobic effect of both the long alkyl chains and the perylene cores, the formed PTCT-DOAB complex precipitated from aqueous solution. When the solution of the anionic PTCTK was added into the solution of a cationic surfactant with a *single* long alkyl side chain (such as octadecyltrimethylammonium bromide), we failed to obtain the corresponding precipitate. We still believe that a complex has formed because the green fluorescence of PTCTK immediately disappeared after mixing with the surfactant, but it is not clear at this time why there was no precipitation.

Solubility

Almost all studies on self-assembly of perylene derivatives have pointed out that their solubility will determine whether they can be applied as key functional materials. Contrary to existing perylene derivatives, our derivatives consist of a perylene core and eight long alkyl chains attached *via* ionic bonds. Thus, their solubility in common organic solvents depends on a balance of nonpolar alkyl chains and polar ionic bonds. The solubility of the complex was tested qualitatively in various organic solvents. PTCT-DOAB can easily dissolve in methanol (dielectric constant ε = 31.2), ethanol (25.7), dichloromethane (9.1) and chloroform (4.9) under ambient conditions, and is soluble in toluene (2.24) and dimethylformamide (36.71) at about 50 °C. It has a very low solubility in *n*-hexane (1.89), diethyl ether (4.197), tetrahydrofuran (7.58) and ethyl acetate (6.02), and is insoluble in water (80.1) and acetone (20.7).

Clearly, PTCT-DOAB can dissolve in many organic solvents. Its dissolution behavior appears to be quite complicated because of the strong amphiphilic nature of these complexes. On the one hand, the long alkyl chains increase the affinity of the complex towards nonpolar compounds, so that

PTCT-DOAB is able to dissolve in various nonpolar solvents such as chloroform and toluene. On the other hand, the existence of ionic bonds increases the interaction between the complex and polar compounds, so that PTCT-DOAB is also able to dissolve in some polar solvents such as methanol, ethanol and dimethylformamide. An interesting phenomenon is that PTCT-DOAB could completely dissolve in tetrahydrofuran once a drop of water was added.

Aggregate morphology

Fig. 1 presents POM and SEM images showing the morphology of as-prepared PTCT-DOAB aggregates (denoted as PTCT-DOAB-1) which both show rectangular platelets with a length and a width in the range of several to a couple of tens of micrometers. In Fig. 1(b) the POM image, which was obtained under crossed polarizers, shows the optical anisotropy of the aggregates. The image indicates an ordered anisotropic structure existing in the aggregates. In Fig. 1(d) the SEM image reveals that the platelets are composed of thinner layers, suggesting that these aggregates may possess a lamellar structure. The precipitation of PTCT-DOAB from water is expected to be a self-assembly process owing to the strong π–π stacking of the perylene cores and the hydrophobic interactions of the alkyl chains with solvents. The formation of these regular aggregates explains why the complex product is stoichiometric and has an extremely high purity.

In our work we found that the preparation of the ordered aggregates is reproducible under controlled conditions. Two different binary solvent systems were used to prepare the assembled PTCT-DOAB complex. Ethanol (ε = 25.7) is a good solvent while water (ε = 80.1) is a poor solvent for the PTCT-DOAB complex. Therefore, we could produce ordered PTCT-DOAB aggregates by changing the solvent from ethanol to an ethanol–water mixture because of the miscibility between alcohol and water. In our experiment we used a method reported in previous studies.[8f] A small volume (100 μL) of concentrated ethanol solution (0.5 mM) of PTCT-DOAB was injected into a large volume of water (1 mL). Due to the hydrophobicity of the long alkyl chains the solubility of the PTCT-DOAB complexes in the mixed solvent is lower than that in ethanol. In the experiment we observed that the solution color turned from green to orange and the aggregates dispersed in the mixed solvent. In such an environment, it is the strong π–π interaction that leads to the self-assembly of the PTCT-DOAB complexes into ordered aggregates (denoted as PTCT-DOAB-2). Fig. 2 shows a set of images of the PTCT-DOAB-2 aggregates obtained using POM, SEM and TEM. These images show extended prism or needle-like features with an average length of 100 μm and an average width of 5 μm. In Fig. 2(b) the POM image obtained under the crossed polarizers shows the optical anisotropy of the aggregates. In Fig. 2(d) the TEM image displays the ribbon nature of the aggregates.

In another experiment we selected a toluene–acetone mixture to create the ordered aggregates. In our experiment the same approach was used: A small volume (100 μL) of concentrated toluene solution (0.5 mM) of PTCT-DOAB was injected into a large volume of acetone (1 mL). The poor interaction between the alkyl chains and the solvent molecules resulted in an assembly of the PTCT-DOAB complexes in the mixed solvent. Fig. 3 shows another set of POM, SEM and TEM images of the aggregates (denoted as PTCT-DOAB-3). These images also show the needle shape and the optical anisotropy of the aggregates.

Previous studies have reported the successful fabrication of nanobelts from some PTCDI derivatives with short and linear alkyl chains in various common solvents.[8f] These previous studies also showed that long and/or branched alkyl side chains can weaken the π–π stacking interaction of the perylene disks, so that the formation of the semiconducting 1D columnar structures is more difficult. Therefore, it is interesting to note that the PTCT-DOAB complex still demonstrates a strong structure-forming ability despite its long alkyl side chains. This may be a promising perylene derivative which could be applied as a functional material with a highly ordered 1D columnar structure.

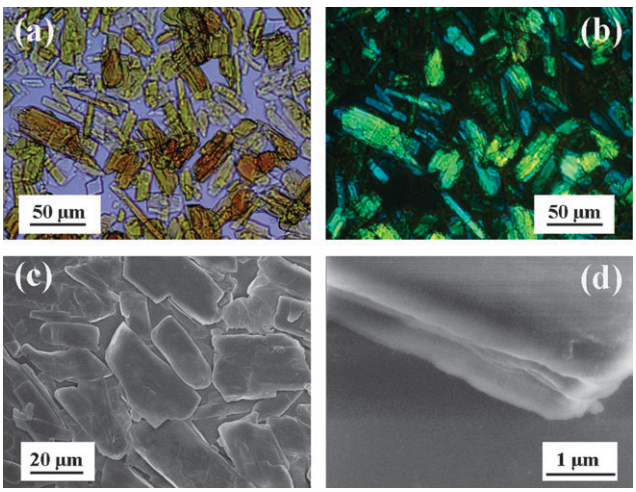

Fig. 1 Morphology of as-prepared PTCT-DOAB-1: (a) POM image, (b) POM image under crossed polarizers, (c) SEM image and (d) higher-magnification SEM image over an aggregate.

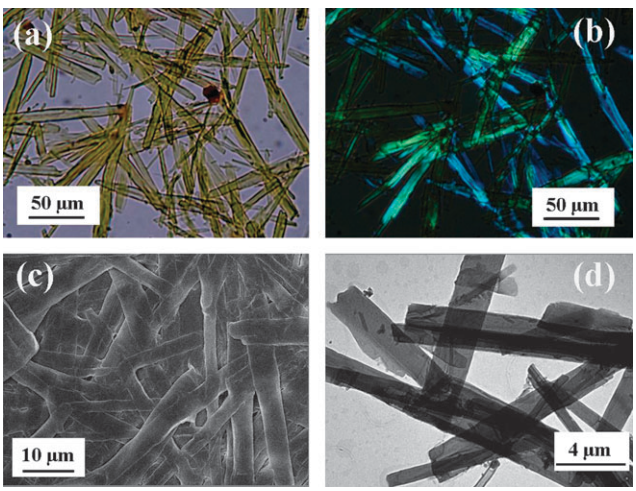

Fig. 2 Aggregate morphology of PTCT-DOAB-2 prepared from a mixed solvent of ethanol and water. (a) POM image, (b) POM image under crossed polarizers, (c) SEM image and (d) TEM image.

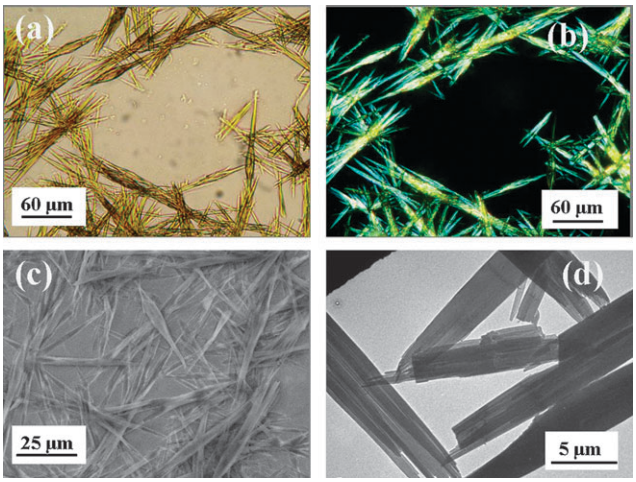

Fig. 3 Aggregate morphology of PTCT-DOAB-3 prepared from a mixed solvent of toluene and acetone. (a) POM image, (b) POM image under crossed polarizers, (c) SEM image and (d) TEM image.

Ultralong aggregates

In a nucleation-growth process, the aggregate size depends on several kinetic factors. It is understandable that ultralong aggregates could be created under conditions near the equilibrium from the view point of crystallization kinetics. In our work, we prepared ultralong aggregates (denoted as PTCT-DHAB-4) when we cooled a toluene solution of PTCT-DHAB from about 50 °C to room temperature and then allowed the solvent to evaporate very slowly. Under these mild conditions, the aggregates could grow through a slow process mainly along the axis of the long aggregates. Fig. 4 shows the POM and SEM experimental evidence found in a sample treated under the conditions mentioned above for a period of about two months. Our measurement showed that the average length is more than 4 mm (exceeding the size of the scan frame). The width of these aggregates varies in a range of 1–10 μm, as shown by the SEM images obtained at different magnifications in Fig. 4(c) and (d). We can see a typical ribbon-like morphology.

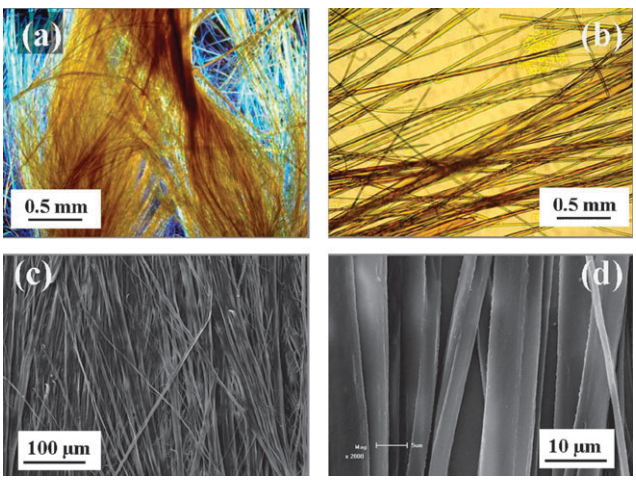

Fig. 4 Ultralong ribbon-like aggregates of PTCT-DHAB-4 prepared by slow evaporation of toluene. (a) POM image, (b) POM image under crossed polarizers, (c) SEM image and (d) higher-magnification SEM image.

Packing behavior in the aggregates or crystals

The molecular order of these complexes with needle-like aggregates or crystals was determined by XRD. Fig. 5(a) shows an anisotropic WAXS pattern of the PTCT-DOAB-2 crystals with the needle axes preferentially oriented about the vertical direction. Fig. 5(b) shows the corresponding powder scattering curve as a function of the absolute value of the scattering vector $s = (2\sin\theta)/\lambda$ where λ is the wavelength and 2θ is the scattering angle between incident and scattered beam. Since the irradiated volume covered a large number of slightly misaligned needle-shape crystals, we assume the presence of simple fiber symmetry with a finite degree of preferred orientation which is supported by the typical arc-shape of the observed reflections. Thus, we will refer the vertical direction as the meridian and to the horizontal direction as the equator, respectively.

At small angles, the scattering pattern is dominated by the strong equidistant reflections observed on the meridian at multiples of $s = 0.222$ nm^{-1}, corresponding to a Bragg spacing of $d = 4.50$ nm. The equidistant nature of this series of reflections indicates a highly ordered layered arrangement with the corresponding period that is aligned with the layer normal pointing in the direction of the needle axis.

As estimated from molecular modeling (MM2 force field, Fig. 6(a)), the length of the perylene part is around 1.2 nm, and the width about 0.68 nm. The length of the alkyl chains in an all-*trans* conformation is about 2.4 nm. As a result, the total length of a fully stretched PTCT-DOAB complex amounts to about 6.0 nm, and the lateral dimension of the perylene core amounts to about 0.68 nm. The fact that we still observe sharp peaks at high angles rather than a broad amorphous halo indicates that the alkyl chains are also arranged in a regular packing, with a fully stretched all-*trans* conformation being the most likely one. However, the calculated length of 6.0 nm is quite a bit longer than the observed Bragg spacing of 4.5 nm of the layered structure. At first sight, this suggests a smectic-C-like tilt of the molecules to account for the needed reduction in the repeat spacing. However, a closer inspection of the WAXS pattern shows that such a straightforward model is not sufficient to explain its features. Revisiting the equidistant meridional reflections we notice the curiously low intensity of the 2nd and 4th order reflections, *i.e.*, the even

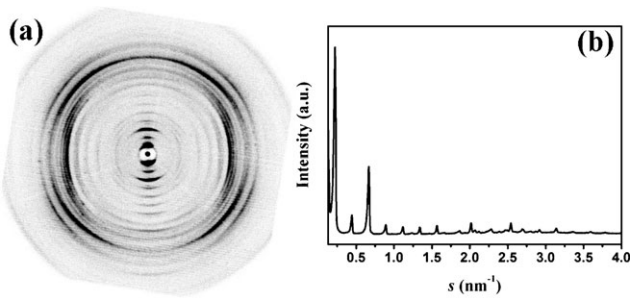

Fig. 5 (a) Experimental 2D-WAXS pattern and (b) X-ray diffraction pattern of PTCT-DOAB-2.

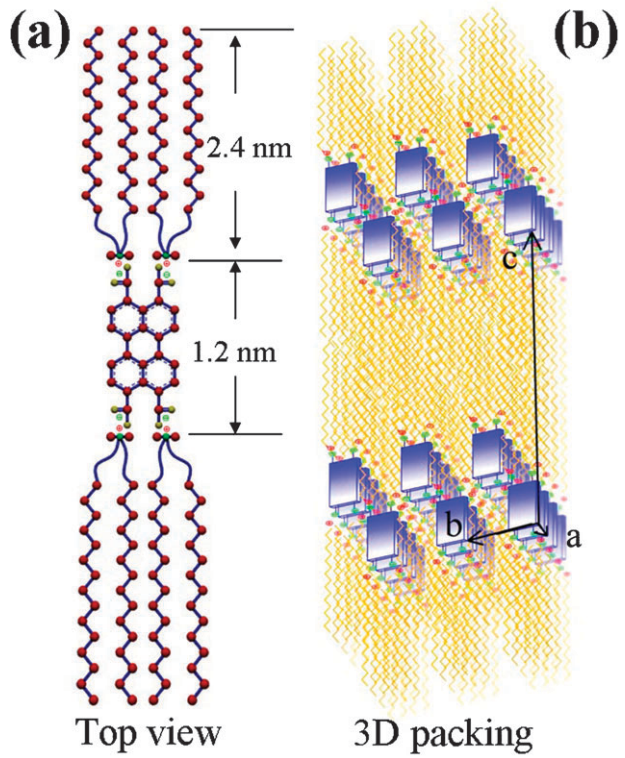

Fig. 6 Schematic illustration of the packing of PTCT-DOAB-2.

order reflections, compared to that of the 1st and 3rd order reflections. This pattern is typically observed for a close-to-symmetric lamellar system, *i.e.*, when the thicknesses of the two types of stacked layers are very close to each other. For a perfectly symmetric square-well density profile, *i.e.*, exact identity of the two thicknesses, the even orders would be extinct. However, now we have a problem: the length of the perylene unit (1.2 nm) is not even close to one half of the observed period of 4.5 nm. Thus, a straightforward tilted layering with a tilt adjusted to generate the correct spacing would result in a much higher intensity for the even meridional orders than is experimentally observed. In order to resolve this contradiction, it is crucial to understand that the intensity section along the meridian depends only on the projection of the total electron density distribution onto the fiber axis but not on any details of the lateral arrangement of the structural units which could only manifest itself in the equatorial or off-axis regions of the scattering pattern. The easiest way to create a close-to-symmetric square-well density profile in the projection onto the fiber axis is the staggered arrangement sketched in Fig. 6(b). We immediately notice that the combined length of two 1.2 nm perylene units is indeed close to one half of the observed 4.5 nm period, with the difference being accountable to both the exact value of the relative shift of the staggered units and a small tilt that still should be present. Thinking about reasons for this staggered arrangement and about the chemical nature of the region of contact between diagonally neighboring perylene units suggests that the four quaternary ammonium cations are forming bridges between the carboxylic anions, as is sketched in Fig. 6(b). Note that the proposed structure is still charge neutral.

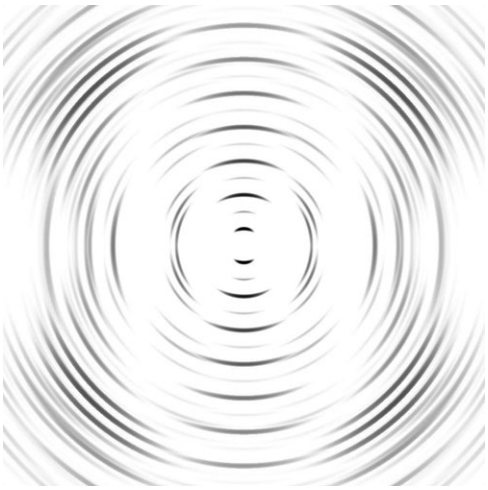

Fig. 7 Calculated WAXS pattern of PTCT-DOAB-2.

In an attempt to semi-quantitatively reproduce the essential features of the experimental 2D WAXS pattern, we used a monoclinic unit cell with cell parameters $a = 0.496$ nm, $b = 1.17$ nm, $c = 6.37$ nm, $\beta = 135°$, where the combination of a and β is adjusted to generate a perylene-to-perylene (π–π) spacing of 0.35 nm, b should be about twice the lateral width of the perylene units, and c should be a little longer than the stretched complex length. The contents of the unit cell were simply approximated by two rectangular platelets representing the perylene units. Any further details of the chemical structure were neglected. Fig. 7 shows a calculated WAXS fiber pattern based on this simple model where the degree of preferred orientation was adjusted to a Hermans' orientation parameter of 0.96. It can be seen that the calculated pattern at least qualitatively reproduces the various relative intensity differences observed in the experimental pattern (Fig. 5(a)), in particular the characteristic intensity sequence of the equidistant reflections on the meridian. The remaining differences indicate the potential for a further refinement of this structure investigation which is, however, hampered by the limited availability of the experimental 2D setup.

We also determined the XRD pattern for PTCT-DOAB-3 as shown in Fig. 8. Only one set of Bragg peaks (with a spacing ratio of 1 : 2 : 3) was found that has also shifted to a larger angle compared to that of PTCT-DOAB-2, resulting in a smaller value for the long period of 3.0 nm. Note also that now the 2nd order is much stronger than the 3rd order reflection, indicating that this structure does not form staggered layers but only simple layers of the perylene groups. The inset does not show any sharp reflections at large s, only a faint amorphous halo. Thus, the aliphatic C18 chains of DOAB are not crystallized but rather molten, *i.e.*, they are not stretched all-*trans* but form more or less random coils. This leads to a reduction of the long period as observed in the experiment. The spacing reduction due to the aliphatic chain conformation is to be combined with a spacing reduction due to the tilt of the perylene disks for which there is evidence from the fluorescence data as discussed below. The combined effects are sketched in Fig. 9. Comparing with the arrangement of PTCT-DOAB-2, we observe that PTCT-DOAB-3 still forms a

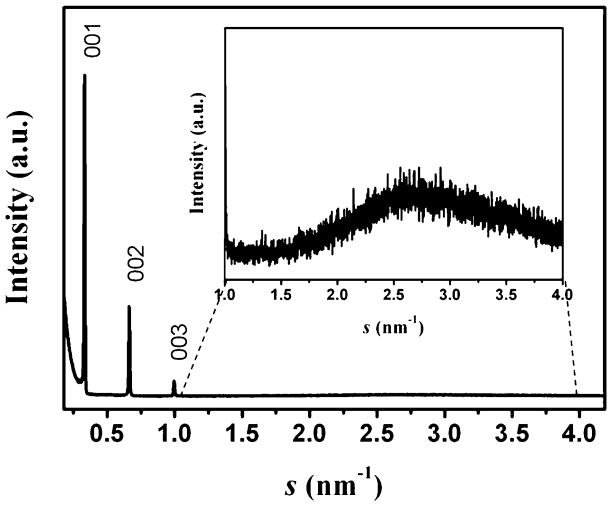

Fig. 8 X-Ray diffraction patterns of PTCT-DOAB-3.

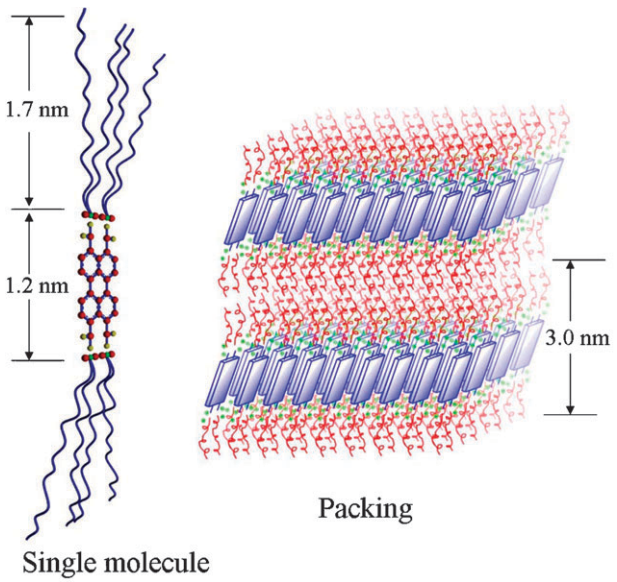

Fig. 9 Schematic illustration of the packing of PTCT-DOAB-3 precipitated from toluene solution with acetone.

highly ordered lamellar structure, even though the alkyl chains appear as random coils. The absence of the expected scattering due to the here still present regular perylene columnar stacking must be attributed to orientation effects, *i.e.*, they would be observed in a 2D WAXS experiment, but the for the present 1D WAXS experiment the orientation of the anisotropic sample precluded their observation. Thus, in PTCT-DOAB-3 there are two levels of regular order, the columnar stacking of the perylene units and the lamellar stacking of perylene layers, with the remaining parts showing a liquid-like disorder.

Spectra characterization

The optical properties of perylene derivatives have also attracted wide investigation, as these chromophores show excellent properties in light absorption and emission, which are greatly influenced by their supramolecular structures. The

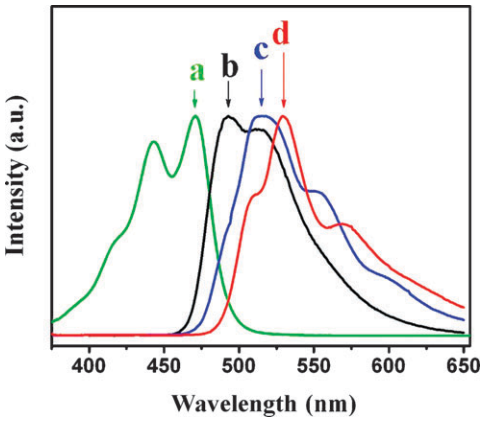

Fig. 10 UV-Vis absorption spectra (a) and fluorescence spectra (b) of dilute ethanol solutions of PTCT-DOAB, and fluorescence spectra of PTCT-DOAB-2 (c) and PTCT-DOAB-3 (d) solid state films. All the spectra are normalized.

fundamental understanding of the correlation between optical properties and molecular arrangement in supramolecular aggregates has been studied.[17] The UV/Vis absorption spectrum of PTCT-DOAB at low concentration in ethanol (the green curve in Fig. 10) shows two pronounced peaks at *ca.* 471 and 443 nm and one weak shoulder around 416 and 391 nm, which correspond to the 0–0, 0–1, 0–2 and 0–3 electronic transitions, respectively. The ethanol solution of this complex shows a bright green fluorescence, even under daylight. The normalized fluorescence spectrum at a low concentration in ethanol (the black curve in Fig. 10) resembles the mirror image of the corresponding to UV/Vis absorption spectra, which can be well assigned to the emission of the monomeric complex. The spectra clearly show strong emission with two maxima at 492 and 513 nm, which are longer than the absorption wavelength. Also, the fluorescence of the PTCT-DOAB solid film with different long periods was studied. The fluorescence spectra of solid PTCT-DOAB-2 (with longer molecular spacing) shows two peaks centered at 516 and 552 nm (the blue curve in Fig. 10) and that of PTCT-DOAB-3 (with shorter molecular spacing) also shows two peaks at 529 and 570 nm (the red curve in Fig. 10), which are blue-shifted compared to other perylene derivatives. The fluorescence maxima of the dilute solutions show a red shift of about 22 nm with respect to the absorption band. This is because the energy of the fluorescence emission is lower than that of the absorption, which is ascribed to the energy loss in the fluorescence emission due to internal conversion and vibration relaxation. However, the solid film fluorescence of both PTCT-DOAB-2 and PTCT-DOAB-3 is red-shifted with respect to the fluorescence of the solutions. We attribute this shift to the formation of excimers as this is observed in other compounds containing the same chromophores. In the aggregate state, when a monomer molecule absorbs a photon, it is electronically excited and excitonic coupling with the neighbor unexcited chromophore may take place. In this situation, excimers are formed, which leads to the increase of the ground state energy and to the decrease of the excited state energy compared to the monomer species, causing a red shift of the aggregate fluorescence.

More interestingly, the emission wavelengths of PTCT-DOAB with the different molecular spacings are different from each other: PTCT-DOAB-3 is further red-shifted by 13 nm compared to PTCT-DOAB-2. The energy level of the ground state of the two monomers increases with decreasing distance between the two monomer molecules. Therefore, a shorter distance should lead to a red shift of the fluorescence according to the energy level diagram.[17b] The shorter intermolecular spacing of PTCT-DOAB-3 compared to PTCT-DOAB-2 may be caused by two aspects, the random coils of the aliphatic C18 chains (see above) and the tilt of the stacking of the perylene cores. The latter means that PTCT-DOAB-3 has a larger longitudinal offset of the perylene cores, which also leads to a red shift of the emission. So, we can see the overall rule that the maxima bands are red-shifted as the intermolecular spacing decreases.

Conclusions

In this study we have presented an extremely facile one-pot method to synthesize a novel kind of perylene derivatives, PTCT-DOAB and PTCT-DHAB, *via* the complexation of a perylene-based anionic core with a cationic surfactant in water. Pure complexes could be obtained in high yield, within a short time, at room temperature, and in water, an environment-friendly solvent. This is particularly interesting as the synthesis of most PTCDA derivatives by conventional methods often requires rather severe conditions. The as-synthesized PTCT-DOAB and PTCT-DHAB complexes are highly soluble in various solvents such as methanol and ethanol, and their solutions show strong fluorescence emissions. With the cooperative action of alkyl chain interaction, perylene core π–π stacking and ionic interaction, the complexes are able to aggregate in a highly ordered fashion. The self-assembly of PTCT-DOAB and PTCT-DHAB complexes in solution leads to the formation of needle-like aggregates in ethanol–water or toluene–acetone binary solvents. PTCT-DHAB ultralong ribbons were obtained by slow evaporation of the toluene solution. XRD measurements showed that well-defined layered structures exist in these aggregates, which are differing primarily by the degree of order in the alkyl part, leading to different long periods and resulting in different fluorescence behavior in the solid state. The fluorescence maxima of complexes with shorter long periods are red-shifted compared to those with longer long periods. We hope to see that our results concerning the highly ordered structures of the complexes can evoke some investigations on their functionality.

Experimental

Materials

PTCDA and the cationic surfactants with two long alkyl side chains, DOAB and DHAB, were purchased from Aldrich. Potassium hydroxide (85%) and organic solvents (AR) were purchased from Keruisi Company, China. They were all used as received. Deionized water was used in the preparation of all complexes.

Instrumentation and characterization

^{1}H nuclear magnetic resonance (^{1}H NMR) spectra were recorded in CD_3OD on a Varian Unity-plus 400 spectrometer with TMS as internal standard at room temperature. For Fourier transform infrared spectroscopy (FT-IR) measurements a Bio-Rad FTS-6000 FT-IR spectrometer was used. Potassium atomic absorption analyses were performed using Shimadzu AA-6800F spectrometer. The amount of Br^- was monitored by a Dionex DX-120 ion chromatograph. The X-ray diffraction (XRD) patterns were measured using a Rigaku D/Max-2500 X-ray diffractometer, equipped with a copper rotating anode source operated at 40 kV/100 mA. 2D-WAXS experiments were performed on a WAXS system at the Max-Planck-Institute for Polymer Research of Germany. The system is composed of a two-dimensional detector (Bruker-AXS HiStar 1024 × 1024 pixels, 100 mm), a mirror (Osmic) and an X-ray generator (AXS 760H) operated at 35 kV and 30 mA. The recording time for each measurement was 1800 s. The distance between the sample and the detector was 75 mm. For both XRD setups, the wavelength of the incident X-ray beam from Cu-Kα radiation was λ = 0.154 nm. UV-Vis absorption spectra were recorded on a VARIAN Cary 300 spectrophotometer using a quartz cell with a path length of 10 mm. Solution fluorescence spectra were obtained with a VARIAN Cary Eclipse fluorimeter and fluorescence spectra of solid samples on a SPEX FL-210 spectrofluorometer. Polarized optical microscopy (POM) experiments were performed using a BX51 Olympus optical microscope equipped with a digital camera. Scanning electron microscopy (SEM) experiments were conducted on a JEOL JSM-6700F field emission SEM. The samples were coated with gold prior to analysis. Transmission electron microscopy (TEM) images were recorded using a Tecnai-G220 transmission electron microscope operated at an accelerating voltage of 200 kV. The samples were prepared by casting the suspension of the complexes onto carbon film-coated copper grids, followed by drying in air.

Synthesis

The perylene derivatives were prepared by simply allowing stoichiometric amounts of PTCTK and DOAB or DHAB to form complexes in solution. The product is denoted as PTCT-DOAB or PTCT-DHAB, respectively in this study. Typical synthesis processes are given below.

For the production of PTCT-DOAB, 39.2 mg PTCDA (0.1 mmol) was at first dissolved in 20 mL KOH aqueous solution (30 mM) at elevated temperature (*e.g.* 50 °C), and the anhydride group was hydrolyzed to yield the potassium salt (PTCTK). When PTCDA was completely dissolved, the PTCTK solution was cooled to room temperature. The DOAB solution was prepared by dissolving 252.4 mg DOAB (0.4 mmol) in 20 mL binary solvent of water–ethanol (volume ratio 1 : 1) (the solubility of DOAB is very low in water but is high in the mixture of water and ethanol). Adding the PTCTK solution into the DOAB solution at room temperature immediately formed a charge stoichiometric complex which was precipitated from solution. The precipitate was isolated by filtration, and the solid was washed with a mixture of water

and ethanol (1 : 1) several times to remove any remaining inorganic salt or physisorbed surfactants. The complex was dried under vacuum at room temperature, resulting in an orange powder with a yield of 98.5%. ^{1}H NMR measurements and elemental analysis (potassium, bromide) indicated that stoichiometric ratio of the complexation was achieved, which also excluded the presence of significant amounts of free surfactant or uncomplexed PTCTK molecules in the solid precipitate. ^{1}H NMR (CD_3OD): δ 0.90 (t, 24H, $8CH_3$), 1.29 (m, 240H, $120CH_2$), 1.68 (m, 16H, $8CH_2$), 3.01 (s, 24H, $8CH_3$), 3.21 (m, 16H, $8CH_2$), 7.87 and 8.29 (each d, 8H, perylene). FTIR (KBr, cm^{-1}): (N^+-^-O) 3028, (C–H) 2920, (C–H) 2850, (Ar) 1598, (COO^-) 1560, (CH_2, CH_3) 1470, (COO^-) 1419, (Ar) 1388, (Ar) 1358, (Ar–H) 1203, (Ar–H) 810, (Ar–H) 779, (CH_2) 720.

The preparation of PTCT-DHAB was similar to that of PTCT-DOAB and the yield was 97.9%. ^{1}H NMR (CD_3OD): δ 0.90 (t, 24H, $8CH_3$), 1.29 (m, 240H, $120CH_2$), 1.68 (m, 16H, $8CH_2$), 3.01 (s, 24H, $8CH_3$), 3.21 (m, 16H, $8CH_2$), 7.87 and 8.29 (each d, 8H, perylene). FTIR (KBr, cm^{-1}): (N^+-^-O) 3028, (C–H) 2920, (C–H) 2850, (Ar) 1598, (COO^-) 1560, (CH_2, CH_3) 1470, (COO^-) 1419, (Ar) 1388, (Ar) 1358, (Ar–H) 1203, (Ar–H) 810, (Ar–H) 779, (CH_2) 720.

Acknowledgements

This work was supported by the National Science Foundation of China (NSFC Grant Nos. 20374030 and 20734001).

References

1 For a review on organic and polymeric semiconductors with 1D nanostructures, see: (*a*) A. P. H. J. Schenning and E. W. Meijer, *Chem. Commun*., 2005, 3245–3258; (*b*) F. J. M. Hoeben, P. Jonkheijm, E. W. Meijer and A. P. H. J. Schenning, *Chem. Rev*., 2005, **105**, 1491–1546; (*c*) J. Wu, W. Pisula and K. Müllen, *Chem. Rev*., 2007, **107**, 718–747; (*d*) A. L. Briseno, S. C. B. Mannsfeld, S. A. Jenekhe, Z. Bao and Y. Xia, *Mater. Today*, 2008, **11**, 38–47.

2 L. Schmidt-Mende, A. Fechtenkotter, K. Müllen, E. Moons, R. H. Friend and J. D. MacKenzie, *Science*, 2001, **293**, 1119–1122.

3 M. D. Curtis, J. Cao and J. W. Kampf, *J. Am. Chem. Soc*., 2004, **126**, 4318–4328.

4 For a review on enhancing the performance of organic and polymeric semiconductors with 1D nanostructure, see: (*a*) J. Cornil, D. Beljonne, J.-P. Calbert and J.-L. Brédas, *Adv. Mater*., 2001, **13**, 1053–1067; (*b*) A. N. Aleshin, *Adv. Mater*., 2006, **18**, 17–27.

5 For a review on synthesis of PTCDIs, see: (*a*) H. Langhals, *Heterocycles*, 1995, **40**, 477–500; (*b*) H. Langhals, *Helv. Chim. Acta*, 2005, **88**, 1309–1343; (*c*) references cited therein.

6 (*a*) R. Stolarski and K. J. Fiksinski, *Dyes Pigm*., 1994, **24**, 295–303; (*b*) S. Benning, H.-S. Kitzerow, H. Bock and M.-F. Achard, *Liq. Cryst*., 2000, **27**, 901–906; (*c*) T. Hassheider, S. A. Benning, H.-S. Kitzerow, M.-F. Achard and H. Bock, *Angew. Chem., Int. Ed*., 2001, **40**, 2060–2063; (*d*) I. Seguy, P. Jolinat, P. Destruel, R. Mamy, H. Allouchi, C. Courseille, M. Cotrait and H. Bock, *ChemPhysChem*, 2001, **7**, 448–452; (*e*) A. Arnaud, J. Belleney, B. Francois, L. Bouteiller, G. Carrot and V. Wintgens, *Angew. Chem., Int. Ed*., 2004, **116**, 1750–1753.

7 (*a*) A. C. Grimsdale and K. Müllen, *Angew. Chem., Int. Ed*., 2005, **44**, 5592–5629; (*b*) A. Herrmann and K. Müllen, *Chem. Lett*., 2006, **35**, 978–985; (*c*) H. Quante, Y. Geerts and K. Müllen, *Chem. Mater*., 1997, **9**, 495–500; (*d*) U. Rohr, P. Schlichting, A. Böhm, M. Gross, K. Meerholz, C. Bräuchle and K. Müllen, *Angew. Chem., Int. Ed*., 1998, **37**, 1434–1437; (*e*) F. Würthner, A. Sautter and J. Schilling, *J. Org. Chem*., 2002, **67**, 3037–5629; (*f*) C. Kohl, T. Weil, J. Qu and K. Müllen, *Chem.–Eur. J*., 2004, **10**, 5297–5310; (*g*) C.-C. You, C. R. Saha-Möller and F. Würthner, *Chem. Commun*., 2004, 2030–2031; (*h*) F. Würthner, V. Stepanenko, Z. Chen, C. R. Saha-Möller, N. Kocher and D. Stalke, *J. Org. Chem*., 2004, **69**, 7933–7939; (*i*) M. G. Debije, Z. Chen, J. Piris, R. B. Neder, M. M. Watson, K. Müllen and F. Würthner, *J. Mater. Chem*., 2005, **15**, 1270–1276; (*j*) S. Müller and K. Müllen, *Chem. Commun*., 2005, 4045–4046; (*k*) S. Y. Chen, Y. Q. Liu, W. F. Qiu, X. Sun, Y. Q. Ma and D. B. Zhu, *Chem. Mater*., 2005, **17**, 2208–2215; (*l*) W. F. Qiu, S. Y. Chen, X. B. Sun, Y. Q. Liu and D. B. Zhu, *Org. Lett*., 2006, **8**, 867–870.

8 (*a*) A review on organization of perylene derivatives, F. Würthner, *Chem. Commun*., 2004, 1564–1579, and references cited therein; (*b*) F. Würthner, C. Thalacker, S. Diele and C. Tschierske, *Chem.–Eur. J*., 2001, **7**, 2245–2253; (*c*) X. Guo, D. Zhang, H. Zhang, Q. Fan, W. Xu, X. Ai, L. Fan and D. Zhu, *Tetrahedron*, 2003, **59**, 4843–4850; (*d*) M.-M. Shi, H.-Z. Chen, Y.-W. Shi, J.-Z. Sun and M. Wang, *J. Phys. Chem. B*, 2004, **108**, 5901–5904; (*e*) J. van Herrikhuyzen, A. Syamakumari, A. P. H. J. Schenning and E. W. Meijer, *J. Am. Chem. Soc*., 2004, **126**, 10021–10027; (*f*) K. Balakrishnan, A. Datar, T. Naddo, J. Huang, R. Oitker, M. Yen, J. Zhao and L. Zang, *J. Am. Chem. Soc*., 2006, **128**, 7390–7398; (*g*) A. L. Briseno, S. C. B. Mannsfeld, C. Reese, J. M. Hancock, Y. Xiong, S. A. Jenekhe, Z. Bao and Y. Xia, *Nano Lett*., 2007, **7**, 2847–2853; (*h*) Z. Chen, V. Stepanenko, V. Dehm, P. Prins, L. D. A. Siebbeles, J. Seibt, P. Marquetand, V. Engel and F. Würthner, *Chem.–Eur. J*., 2007, **13**, 436–449; (*i*) Z. Chen, U. Baumeister, C. Tschierske and F. Würthner, *Chem.–Eur. J*., 2007, **13**, 450–465; (*j*) V. Dehm, Z. Chen, U. Baumeister, P. Prins, L. D. A Siebbeles and F. Würthner, *Org. Lett*., 2007, **9**, 1085–1088; (*k*) G. D. Luca, A. Liscio, P. Maccagnani, F. Nolde, V. Palermo, K. Müllen and P. Samorí, *Adv. Funct. Mater*., 2007, **17**, 3791–3798; (*l*) Y. Xu, S. Leng, C. Xue, R. Sun, J. Pan, J. Ford and S. Jin, *Angew. Chem., Int. Ed*., 2007, **46**, 3896–3899; (*m*) V. Marcon, J. Kirkpatrick, W. Pisula and D. Andrienko, *Phys. Status Solidi B*, 2008, **245**, 820–824.

9 (*a*) A. Syamakumari, A. P. H. J. Schenning and E. W. Meijer, *Chem.–Eur. J*., 2002, **8**, 3353–3361; (*b*) C. Thalacker and F. Würthner, *Adv. Funct. Mater*., 2002, **12**, 209–218; (*c*) A. P. H. J. Schenning, J. van Herrikhuyzen, P. Jonkheijm, Z. Chen, F. Würthner and E. W. Meijer, *J. Am. Chem. Soc*., 2002, **124**, 10252–10253; (*d*) F. Würthner, Z. Chen, F. J. M. Hoeben, P. Osswald, C.-C. You, P. Jonkheijm, J. van Herrikhuyzen, A. P. H. J. Schenning, P. P. A. M. van der Schoot, E. W. Meijer, E. H. A. Beckers, S. C. J. Meskers and R. A. J. Janssen, *J. Am. Chem. Soc*., 2004, **126**, 10611–10618; (*e*) Y. Liu, J. P. Zhuang, H. B. Liu, Y. L. Li, F. S. Lu, H. Y. Gan, T. G. Jiu, N. Wang, X. R. He and D. B. Zhu, *ChemPhysChem*, 2004, **5**, 1210–1215; (*f*) Y. Liu, Y. J. Li, L. Jiang, H. Y. Gan, H. B. Liu, Y. L. Li, J. P. Zhuang, F. S. Lu and D. B. Zhu, *J. Org. Chem*., 2004, **69**, 9049–9054; (*g*) Y. Liu, S. Q. Xiao, H. M. Li, Y. Li, H. B. Liu, F. S. Lu, J. P. Zhuang and D. B. Zhu, *J. Phys. Chem. B*, 2004, **108**, 6256–6260; (*h*) M. E. Canas-Ventura, W. Xiao, D. Wasserfallen, K. Müllen, H. Brune, J. V. Barth and R. Fasel, *Angew. Chem., Int. Ed*., 2007, **46**, 1814–1818; (*i*) B. Jancy and S. K. Asha, *Chem. Mater*., 2008, **20**, 169–181; (*j*) S. Yagai, T. Seki, T. Karatsu, A. Kitamura and F. Würthner, *Angew. Chem., Int. Ed*., 2008, **47**, 3367–3371.

10 (*a*) S.-W. Tam-Chang and I. K. Iverson, *J. Am. Chem. Soc*., 1999, **121**, 5801–5802; (*b*) I. K. Iverson, S. M. Casey, W. Seo and S.-W. Tam-Chang, *Langmuir*, 2002, **18**, 3510–3516; (*c*) S.-W. Tam-Chang, W. Seo, I. K. Iverson and S. M. Casey, *Angew. Chem., Int. Ed*., 2003, **42**, 897–900; (*d*) Y. Guan, Y. Zakrevskyy, J. Stumpe, M. Antonietti and C. F. J. Faul, *Chem. Commun*., 2003, 894–895; (*e*) Y. Zakrevskyy, C. F. J. Faul, Y. Guan and J. Stumpe, *Adv. Funct. Mater*., 2004, **14**, 835–841; (*f*) S.-W. Tam-Chang, W. Seo, K. Rove and S. M. Casey, *Chem. Mater*., 2004, **16**, 1832–1834; (*g*) J. Helbley, I. K. Iverson and S.-W. Tam-Chang, *Langmuir*, 2004, **20**, 342–347; (*h*) Y. Guan, S.-H. Yu, M. Antonietti, C. Böttcher and C. F. J. Faul, *Chem.–Eur. J*., 2005, **11**, 1305–1311; (*i*) A. Xie, B. Liu, J. E. Hall, S. L. Barron and D. A. Higgins, *Langmuir*, 2005, **21**, 4149–4155; (*j*) S.-W. Tam-Chang, J. Helbley, T. D. Carson, W. Seo and I. K. Iverson, *Chem. Commun*., 2006, 503–505; (*k*) D. Franke, M. Vos, M. Antonietti, N. A. J. M. Sommerdijk and C. F. J. Faul, *Chem. Mater*., 2006, **18**, 1839–1847; (*l*) T. A. Everett, A. A. Twite, A. Xie, S. K. Battina, D. H. Hua and D. A. Higgins, *Chem. Mater*.,

2006, **18**, 5937–5943; (*m*) L. Huang, S.-W. Tam-Chang, W. Seo and K. Rove, *Adv. Mater*., 2007, **19**, 4149–4152; (*n*) T. Ma, C. Li and G. Shi, *Langmuir*, 2008, **24**, 43–48; (*o*) A. Laiho, B. M. Smarsly, C. F. J. Faul and O. Ikkala, *Adv. Funct. Mater*., 2008, **18**, 1890–1897; (*p*) S.-W. Tam-Chang, J. Helbley and I. K. Iverson, *Langmuir*, 2008, **24**, 2133–2139.

11 (*a*) R. A. Cormier and B. A. Gregg, *J. Phys. Chem. B*, 1997, **101**, 11004–11006; (*b*) R. A. Cormier and B. A. Gregg, *Chem. Mater*., 1998, **10**, 1309–1319; (*c*) H. Langhals, W. Jona, F. Einsiedl and S. Wohnlich, *Adv. Mater*., 1998, **10**, 1022–1024; (*d*) B. A. Gregg and R. A. Cormier, *J. Am. Chem. Soc*., 2001, **123**, 7959–7960; (*e*) S.-G. Liu, G. Sui, R. A. Cormier, R. M. Leblanc and B. A. Gregg, *J. Phys. Chem. B*, 2002, **106**, 1307–1315; (*f*) W. Wang, L.-S. Li, G. Helms, H.-H. Zhou and A. D. Q. Li, *J. Am. Chem. Soc*., 2003, **125**, 1120–1121; (*g*) W. Wang, J. J. Han, L.-S. Li, E. J. Shaw and A. D. Q. Li, *Nano Lett*., 2003, **3**, 455–458; (*h*) A. D. Q. Li, W. Wang and L.-Q. Wang, *Chem.–Eur. J*., 2003, **9**, 4594–4601; (*i*) A. Datar, R. Oitker and L. Zang, *Chem. Commun*., 2006, 1649–1651; (*j*) Y. Che, A. Datar, X. Yang, T. Naddo, J. Zhao and L. Zang, *J. Am. Chem. Soc*., 2007, **129**, 6354–6355; (*k*) K. Balakrishnan, A. Datar, R. Oitker, H. Chen, J. Zuo and L. Zang, *J. Am. Chem. Soc*., 2005, **127**, 10496–10497.

12 (*a*) X. Zhang, Z. Chen and F. Würthner, *J. Am. Chem. Soc*., 2007, **129**, 4886–4887; (*b*) Y. Che, A. Datar, K. Balakrishnan and L. Zang, *J. Am. Chem. Soc*., 2007, **129**, 7234–7235.

13 (*a*) F. Würthner, A. Sautter, D. Schmid and P. J. A. Weber, *Chem.–Eur. J*., 2001, **7**, 894–902; (*b*) C.-C. You and F. Würthner, *J. Am. Chem. Soc*., 2003, **125**, 9716–9725; (*c*) C.-C. You, C. Hippius, M. Grüne and F. Würthner, *Chem.–Eur. J*., 2006, **12**, 7510–7519; (*d*) F. Würthner, V. Stepanenko and A. Sautter, *Angew. Chem., Int. Ed*., 2006, **45**, 1939–1942.

14 K. Sugiyasu, N. Fujita and S. Shinkai, *Angew. Chem., Int. Ed*., 2004, **43**, 1229–1233.

15 For a review on ISA, see: (*a*) C. K. Ober and G. Wegner, *Adv. Mater*., 1997, **9**, 17–31; (*b*) S. Q Zhou and B. Chu, *Adv. Mater*., 2000, **12**, 545–556; (*c*) C. F. J. Faul and M. Antonietti, *Adv. Mater*., 2003, **15**, 673–683.

16 (*a*) Y. Guan, M. Antonietti and C. F. J. Faul, *Langmuir*, 2002, **18**, 5939–5945; (*b*) Y. Guan, S.-H. Yu, M. Antonietti, C. Böttcher and C. F. J. Faul, *Chem.–Eur. J*., 2002, **8**, 2764–2768; (*c*) Z. Wei, T. Laitinen, B. Smarsly, O. Ikkala and C. F. J. Faul, *Angew. Chem., Int. Ed*., 2005, **44**, 751–756; (*d*) Y. Zakrevskyy, J. Stumpe and C. F. J. Faul, *Adv. Mater*., 2006, **18**, 2133–2136; (*e*) F. Camerel, G. Ulrich, J. Barberá and R. Ziessel, *Chem.–Eur. J*., 2007, **13**, 2189–2200.

17 (*a*) R. F. Fink, J. Seibt, V. Engel, M. Renz, M. Kaupp, S. Lochbrunner, H.-M. Zhao, J. Pfister, F. Würthner and B. Engels, *J. Am. Chem. Soc*., 2008, **130**, 12858–12859; (*b*) B. Stevens and M. I. Ban, *Trans. Faraday Soc*., 1964, **60**, 1515–1523.

